EXPERIMENTAL SEISMIC PERFORMANCE EVALUATION OF THE UNREINFORCED BRICK MASONRY SHEAR WALLS

Mohammed Javed*, Guido Magenes**, Bashir Alam*, Akhtar Naeem*, Qaisar Ali*, Naveed Ahmed ***

* *Department of Civil Engineering, University of Engineering & Technology, Peshawar, 25120, Pakistan*

** *Department of Structural Mechanics, University of Pavia, and EUCENTRE, via Ferrata 1, Pavia, Italy*

*** *ROSE school, University of Pavia, via Ferrata 1, Pavia, Italy*

ABSTRACT

An experimental study to evaluate the seismic performance of unreinforced brick masonry (URBM) shear walls constructed in a special type of mortar being widely used in Northern Pakistan is presented. In-plane shear-compression tests were carried out on twelve walls, using quasi-static cyclic loading. Testing set produced double bending curvature in walls. The effect of aspect ratio and pre-compression levels on various parameters used to quantify seismic performance is examined. Experimental work showed that walls with medium to high aspect ratios failed in diagonal tensile shear failure mode while squat walls failed in diagonal tension shear followed by bed-joint sliding. The diagonal tensile shear strengths of the walls determined from experimental work were then compared with Turnšek and Sheppard equation used to determine diagonal tensile shear strength of URBM walls. Influence of the pre-compression level on the ultimate ductility and drift ratio of the walls and on their equivalent viscous damping is discussed. Finally drift ratios for performance levels corresponding to various damage levels, for unreinforced brick masonry walls, are proposed on the basis of experimental results

Keywords: Unreinforced masonry, Shear strength, Ductility, Drift, Energy dissipation, Performance levels

1. Introduction:

An earthquake jolted Kashmir and the Northern Areas of Pakistan on October 8, 2005. It was one of the deadliest earthquakes (with M_w = 7.6) considering the number of fatalities in the history of indo-Pakistan subcontinent. As a consequence of earthquake, more than 70,000 people died; 80,000 left injured, 2.5 million people were displaced and 3.3 to 3.5 million people were affected. The resulting total economic loss was estimated US$5.2 billion. According to the Asian Development Bank and the World Bank, 4,55,000 buildings were partially or fully damaged. Most of these damaged and collapsed buildings had been constructed with unreinforced stone and brick masonry. However, the performance of unreinforced brick masonry (URBM) was found to be much better than unreinforced stone masonry [1]

The disaster demanded to take the appropriate measures in order to minimize losses against future seismic activities. However, in order to reduce potential damage to structures, a comprehensive seismic risk assessment, a combination of seismic hazard and seismic vulnerability, was needed. The seismic hazard depends upon geology of the area and, therefore, cannot be controlled. However, seismic vulnerability of structures against future seismic activities can be reduced by implementing remedial measures, once the existing seismic vulnerability of buildings located in the area under interest is known. It was, therefore, necessary to assess the seismic vulnerability of existing building stock of Northern Pakistan. As a part of this work [2], experimental work was carried out to evaluate the seismic performance of existing URBM buildings stock of Northern Pakistan and is elaborated in subsequent section. It is important to note that the unreinforced masonry distinguishes itself from other types of construction most obviously by the terrific diversity of its ingredients, and the importance of their interaction in the interpretation

of structural response. The properties of individual components (brick and mortar) and, more importantly, their interaction must be understood before the behaviour of components or structural system can be visualized. Although significant experimental work has been done in the past on concrete, steel structural elements which lead to the well-defined procedures for their seismic design and evaluation, no such consolidated understanding exists about masonry structures.

The research work has led to the development of preliminary analytical tools for the seismic design and assessment of unreinforced masonry (URM) structures (such as FEMA 356 [3] and the subsequent ASCE/SEI 41-06[4], or Eurocode 8 [5]) but still more work needs to be done towards the full understanding of the seismic behaviour of URM structures**.**

It is a known fact that one of the most important factors that influences the behaviour of URBM is mortar. A change in either the constituents and/or proportions of the cementitious material and fine aggregate can induce appreciable changes in the failure mode, lateral load capacity, and deformability of the masonry systems [6]. Thus it is essential to study the behaviour of URBM, made with specific types of mortar. A type of mortar, using stone dust as partial replacement of sand, is widely used in URBM construction throughout Northern Pakistan, however, very little information is available on its behaviour when used in URBM. Therefore, in this work a detailed experimental study was carried out to investigate the seismic performance of URBM shear walls, constructed with stone dust mortar, under the action of in-plane lateral quasi-static cyclic loading. The stone dust is obtained from the crushing industry plants producing coarse aggregates. The stone dust is locally known as '*khaka*'. The name seems to be derived from the word *'khak'*, which means clay.

The entire experimental work was carried out in two phases. In the first phase, tests were conducted to determine the physical and mechanical properties of masonry and its constituents. In the second phase, shear-compression tests were carried out on URBM walls. Aspect ratios and pre-compression levels were varied to observe their effect on the behaviour of the walls. Lateral force-displacement hysteresis diagram of eight walls are presented along with the detailed discussion on the failure modes and cracking pattern. In addition, experimental results regarding displacement ductility and drift capacity, moduli of elasticity and rigidity, energy dissipation characteristics of the tested walls are also discussed and presented in a quantifiable way. The influence of pre-compression level on displacement ductility and energy dissipation characteristics is also investigated.

2. Experimental work

2.1 Properties of masonry and its constituents.

The experimental work was aimed at evaluating the seismic performance of URBM walls constructed in stone dust mortar, being widely used in Northern Pakistan. Unfortunately, testing facilities required for this purpose were not available at the national level when this work was started. The experimental work was, therefore, carried out using the laboratory facilities of the Institute of Engineering Mechanics (IEM) at Harbin, China, using local material available in Harbin city. Best efforts were made to simulate the mechanical properties of brick masonry and its constituents used in Northern Pakistan. As a bench mark, properties of bricks masonry and its constituents used by Ali [7] were considered as standard for this experimental study.

An outline is given in the following sub-sections for the criteria used in the selection of materials for the present study. The results of experiments carried out in this phase are summarized in table 1.

2.1.1 Bricks

The size of solid fired clay bricks used in Harbin was almost similar to those being used in Northern Pakistan. The bricks available in Harbin had no frog, had an average size of 236 x 112 x 53 mm. The ones used in Northern Pakistan, contain a frog, and have an average size of 225 x 110 x 70 mm. The compressive strength of bricks in Harbin was slightly higher than the bricks used in Northern Pakistan. The compressive strength of solid fired clay brick used in Northern Pakistan occasionally exceeds 20 MPa [7]. Bricks used in this experimental study were obtained from a demolished building in Harbin city and had an average compressive strength of 22.5 MPa. These bricks were selected for use as their compressive strength was close to the compressive strength of those commonly used in Northern Pakistan.

2.1.2 Mortar

It is a common practice in Northern Pakistan to use cement: sand: khaka (CSK) mortar in a ratio of 1:4:4 by weight. CSK mortar with the same ratio was used in this experimental work. *Khaka* (i.e., stone dust) was obtained from a stone crushing industry of Harbin. The sieved stone dust was mixed according to the proportions used in the work of Ali [7].

In addition to the ratio requirements of CSK mortar, another benchmark was to achieve a compressive strength of 6.2 MPa at 28 days maturity [7]. For this purpose, CSK mortar cubes with a proportion of 1:4:4 were cast using water/cement (w/c) ratios of 1.1, 1.4 and 1.7 and were tested at the 7 days age. Based on the usual understanding that in 7 days the mortar gains approximately 70% of its 28-days compressive strength, a w/c ratio of 1.1 was found to achieve a target compressive strength of 6.2 MPa at the age of 28 days. However, while casting masonry walls for quasi-static cyclic tests, this mortar was found less workable and thus the w/c ratio was increased to 1.2. The average compressive strength of twenty four mortar cubes having w/c ratio of 1.2 was 5.05 MPa at 28 days.

2.2 Masonry assemblage tests

2.2.1 Compressive strength

Compression tests on masonry prisms were carried out in accordance with ASTM C1314 - 11 standards [8]. The prisms, prepared in CSK 1:4:4 mortar had an average height of 575 mm and an average cross sectional area of 236 mm x 236 mm. Nine prisms were cast using English bond with an average mortar thickness of 10 mm. The prisms were capped on top and bottom ends by using a rich cement sand mortar. All prisms were tested after moist curing for at least 28 days. The average value of the compressive strength of masonry prisms (f_m) was 4.53 MPa.

2.2.2 Modulus of elasticity

The modulus of elasticity of the masonry (E_m) was determined by using the stress-strain data of the masonry prisms tested to determine the compressive strength of masonry according to ASTM C1314 - 11 specifications [8].

Two steel rods, each with flat strips welded at the ends, were inserted in the holes that were drilled at the ends of gauge length, as shown in Figure 1. The vertical displacements at the ends of steel rods were measured using the displacement dial gauges. Difference in the displacements of the two dial gauges provided the shortening in the gauge length. Due to limitations of the testing arrangement, the displacements were not recorded after peak compressive force. However, the recorded data was sufficient enough to determine modulus of elasticity of the masonry prisms. The average value of the modulus of elasticity of the tested masonry prisms was 1300 MPa. The value refers to a secant modulus measured between $0.05f_m$ and $0.333f_m$

2.2.3 Diagonal tensile strength

In order to determine the diagonal tensile strength of masonry (f_{tu}) the diagonal compression tests were carried out in accordance with ASTM E 519 – 02 specifications [9]. Four square panels, each with a side length of 750 mm and thickness of 236 mm were tested using the testing arrangement shown in Figure 2

ASTM specifications do not provide equation to determine the principal tensile strength of masonry. Therefore, the equation recommended by the RILEM specifications [10], was used as follows:

$$f_{tu} = 0.5\frac{(N_D)_u}{A_n} \quad \text{.....} (1)$$

Where $(N_D)_u$ = peak value of the vertical load applied on the masonry prism during the test and A_n = net area of the prism. For solid masonry A_n is the average length of two sides multiplied by the thickness of prism.
The average value of f_{tu} for the masonry prisms, calculated by Equation 1 was 0.24 MPa.

2.2.4 Cohesion and coefficient of friction

No ASTM standard is available to conduct tests on masonry triplet for determining cohesion (c) and coefficient of friction (μ). Therefore, in order to determine the shear strength of the masonry, which depends upon determining cohesion and coefficient of friction, EN-1052-3 specifications [11] were followed to carry out triplets tests. The testing arrangement for these tests is shown in Figure 3**.**
Eleven samples were cast and tested in order to determine c and μ of the masonry triplets. Three specimens were tested without pre-compression. Where, three specimens each were tested under the pre-compression force of 1 and 2 tonne. Two specimens were tested under the pre-compression force of 3 tonne.
Shear strength of a triplet (τ_u) was determined as follows [12]:

$$\tau_u = \frac{V_{us}}{2A_{bm}} \quad \text{.....} \quad (2)$$

where V_{us} = shear force required to produce shear sliding in a triplet, and A_{bm} = area of brick-mortar joint between the two bricks. For a triplet, total area of brick-mortar joints = 2 A_{bm}
Linear regression analysis was carried out in order to determine c and μ, using the experimental data. The regression analysis resulted in values of c = 0.39 MPa and μ = 0.59 with coefficient of determination, r^2=0.827

2.3 In-plane quasi-static cyclic tests on URBM walls

The most important objective of the experimental work was to study the in-plane seismic performance of the solid fired clay brick masonry shear walls constructed in CSK mortar. To accomplish this, shear-compression tests were carried out using quasi-static cyclic loading on four series of walls. The details of testing are given in the following sub-sections.

2.3.1 Geometry of the walls

Walls with three different geometries were tested during experimental work. The walls had the aspect ratios (i.e., height-to-length ratio) of 0.66, 0.93 and 1.22. Three walls each was cast with aspect ratios of 0.66 and 1.22, and the remaining six walls were cast with aspect ratio of 0.93.Keeping in view the capacity of the actuator, the length of each wall was limited to 1360 mm. Nevertheless, the number of courses in each wall specimen is deemed to be sufficiently high to be representative of real walls behaviour.

All walls were constructed using English bond, which is commonly used in Northern Pakistan. The thickness of mortar joints used in Northern Pakistan is approximately 12.5 mm with the bricks having an average thickness of 70 mm. Since the bricks used in the walls had a thickness of 53 mm instead of 70 mm, therefore, the thickness of mortar used in the walls cast for the experimental work was accordingly scaled to 10 mm.

Walls with the aspect ratios of 0.66 and 0.93 were cast to simulate the geometry of typical walls in rooms with a door opening at the end. The walls with an aspect ratio of 1.22 were cast to simulate the geometry of a typical slender pier between door and window openings.

2.3.2 Pre-compression levels

Pre-compression levels on the walls were 0.42, 0.64 and 0.71 MPa. These values of pre-compression simulated the vertical load on walls supporting two to three stories. A total of four series of walls, with three walls in each series, were tested.

Based on the aspect ratio and pre-compression level, walls were divided into four categories, namely WI, WII, WIII and WIV. Each wall in a given series was designated with a lower case alphabet at the end of the category designation. e.g., the first wall of the WI category was designated as WIa. Similarly, the second and the third wall of same category were designated as WIb and WIc, respectively. The details of the dimensions (length, l; thickness, t; height, h), aspect ratios (h/l), and pre-compression levels (σ_o) are given in Table 2.

2.3.3 Testing setup

Quasi-static cyclic tests were carried out for three different levels of pre-compression (σ_o/f_m=0.091, 0.138 and 0.153 corresponding to σ_o= 0.42 MPa, 0.64 MPa and 0.71 MPa, respectively) by using the testing setup shown in Figure 4. The walls at the top and bottom were connected to the stiff reinforced concrete beams using epoxy resin. These reinforced concrete beams were already connected to the frame of testing setup. The vertical pre-compression was developed through two hydraulic jacks in which oil pressure was developed by a manually controlled electric motor. A dial gauge installed on motor allowed monitoring pre-compression on the walls during the testing process. Steel rollers were placed between the jacks and thick steel plates placed above the steel beam connected to the top concrete beam to allow lateral displacement of the wall with minimal friction. The testing setup, as shown in Figure 4, developed double bending curvature in a wall since top beam of testing setup was forced to translate horizontally,

creating a double-fixed condition. In such situation in an ideally homogeneous material the inflection point would be located at mid height of the wall. Experimental work on URBM walls loaded in double bending curvature is less frequent than on cantilever walls since the experimental setup is somewhat more complex. However, in double bending tests it is easier to enforce shear failure mechanisms which are those characterized by lower ductility and displacement capacity which are known to be the most critical parameters for the seismic behaviour of URBM buildings.

The lateral seismic forces were simulated by step wise linearly increasing static lateral displacements. The typical lateral displacement history is shown in Figure 5. The testing process consisted of two phases. The first phase of experimental work on walls was carried out with force controlled testing. This phase consisted of a total of four linearly increasing force cycles of different magnitudes. Objective of the force controlled testing phase was to have a well defined lateral load-displacement curve before the occurrence of diagonal tension shear cracking. The lateral strengths of the walls before testing were estimated by using analytical equations used in the practice. In order to avoid the chances of the formation of diagonal shear cracking in the first phase, the estimated lateral strength of a wall, V_{est}, was taken as 75% of the lateral strength of the wall. Each test was started by applying a lateral force of $V_{est}/4$. A total of three cycles were repeated for this level of force. Each cycle was started by applying the lateral force towards right side, causing a 'push' in the wall. This loading direction was termed as the positive loading direction (PLD). After applying the target force, the pressure in the actuator was gradually decreased to zero and a lateral force with the same magnitude was applied in the reverse direction, causing a 'pull' in the wall and was termed the negative loading direction (NLD). The lateral force was then increased to a magnitude of $V_{est}/2$ and the above mentioned procedure was repeated for three cycles. Similarly, three cycles each were repeated for lateral forces having the magnitudes of ¾ V_{est} and V_{est}. The frequency of loading was kept 1/60 Hz during this phase of testing.

The second phase of experimental work on walls was carried out with displacement controlled testing. The frequency of displacement during this testing phase varied from 1/60 Hz for displacement cycles with lower amplitudes to 1/120 Hz for displacement cycles with higher amplitudes. This phase of testing was started by imposing a lateral displacement slightly higher than the maximum displacement recorded at the end of the force controlled testing phase (multiple of 0.25 mm). Three cycles of the displacement were completed. The next target displacement was imposed by increasing the previous displacement by 0.25 mm. The target displacement was repeated three times. The imposed displacements were incrementally increased by 0.25 mm in each cycle till the amplitude of displacement was 1.0 mm. The increment was kept 0.5 mm for displacement cycles having amplitudes from 1.0 mm to 4.0 mm. The displacement cycles having amplitudes greater than 4.0 mm were increased by 1.0 mm.

Variation in the pre-compression occurred, especially after the diagonal tension cracking in a wall, due to the change in the vertical component of wall's displacement. However, change in pre-compression, which was occasionally more than 4-5%, was instantly controlled by adjusting oil pressure in the hydraulic system.

Deformations in the walls were recorded by means of the LVDTs shown in Figure 4**.** LVDT1 was used to measure the lateral displacement at the top of a wall. LVDT2 was used to monitor possible slippage of a wall with respect to the R.C. beam anchored to the testing floor. LVDT3 was used to check the possibility of rocking, especially in slender walls. LVDT4 and 5 were used to record the diagonal deformations in a wall.

Data of the three wall specimens, namely WIa, WIb and WIIIc, could not be recorded due to some technical problems to the data acquisition system. Similarly, due to vertical stress concentration at the ends, as a result of uneven upper horizontal surface of the wall, data of wall WIVc did not reflect the typical hysteretic behaviour and was, therefore, discarded. Hence, the results of eight out of twelve tested walls are discussed in detail in the paper.

2.4 Cracking pattern and failure modes

As a consequence of the chosen geometry of walls and pre-compression levels, two failure modes, namely diagonal tensile shear cracking and bed joint sliding accompanied by diagonal tensile shear cracking, were observed in the tested walls. Walls with high to medium aspect ratios (WI through WIII), failed in diagonal tension shear without any rocking effect. In the case of squat walls (WIV series) bed joint sliding was observed after the formation of diagonal tension cracks. No rocking was observed in the wall series WIV as well. Detailed discussion on the observed behaviour of walls is given in the following sub-sections:

2.4.1 Wall series WI

Three walls, each having an aspect ratio of 1.22 with pre-compression level of 0.71 MPa, were tested in this series but the data of wall WIa and WIb could not be recorded. In case of walls WIa and WIb the failure mode had been characterized by the formation of diagonal cracks

In case of wall WIc, one main diagonal crack was developed along each direction of lateral loading. As the test progressed, vertical cracks also developed in the middle portion of the wall, as shown in Figure 6. However, in case of wall WIb multiple inclined cracked were produced along both direction of lateral loading as shown in Figure 7

Diagonal cracks in walls WIb and WIc propagated towards top and bottom corners with the increase in lateral displacement. The propagation of these cracks finally led to the crushing of masonry in the walls corners as a result of insufficient area to resist compressive stresses.

2.4.2 Wall series WII

Walls in this series were having an aspect ratio of 0.93 and tested at a pre-compression level of 0.42 MPa. In walls WIIb and WIIc, one of the diagonally cracked wedge shaped portion of wall tended to separate from rest of the wall with the increase in imposed lateral displacement, as shown in Figure 8. In Wall WIIa, a small wedge on the right side got separated from the rest of the wall as shown in Figure 9. With the increase in lateral displacement in NLD the wedge started sliding away from the wall, resulting in a reduction in lateral shear resistance of the wall in NLD as shown in Figure 21b. The lower magnitude of vertical compression may be one of the reasons for such type of behaviour. Splitting of the masonry at the ends, and crushing of masonry at the bottom were also observed in walls.

In spite of little reduction in lateral force after post peak response due to increase in lateral displacements, test was stopped in case of all the three walls as it was felt that the diagonally cracked wedges of walls could fall and might cause damage to the testing set up.

2.4.3 Wall series WIII

Like Walls WII, Walls in this series were also having the aspect ratio of 0.93. However, the pre-compression level was kept 0.64 MPa. The numbers of inclined cracks developed in the walls were relatively more than WII series, as shown in Figures 10 and 11. The damages in WIII series were not localized (i.e., excessive separation of only diagonally cracked wedges as observed in WII series) and were distributed through out each wall, as shown in Figures 10 and 11. Vertical cracks were also observed in the left and right side portions of wall WIIIb, as shown in Figure 11. Extensive crushing of masonry at corners and vertical splitting of masonry at the ends were also observed in the walls, Figure 12. The reason for such type of behaviour may be the relatively higher pre-compression level.

2.4.4 Wall series WIV

Walls in this series were having the lowest aspect ratio of 0.66 and tested under a pre-compression level of 0.64 MPa. Wall WIVc was tested first of all followed by walls WIVa and WIVb. Walls of this series were initially planned to be tested at a pre-compression level of 0.42 MPa. However due to problems in testing of walls WIVc and WIVa it was decided to increase the pre-compression level to 0.64 MPa. The reason for increasing the pre-compression level is given in the following paragraphs.

Wall WIVa was initially tested under a pre-compression of 0.42 MPa. The diagonal tension cracks were developed in both directions of the lateral loading at a lateral displacement of 1.5 mm, Figure 13. However, after the formation of diagonal tension cracks, epoxy resin, which was used to stick the foundation beam of the wall to R.C. beam anchored to the testing floor, failed in shear and the wall slipped at that joint. In order to avoid re-occurring of slippage, testing of wall WIVa was restarted at an increasing pre-compression level of 0.64 MPa. Sliding of the bed joint occurred at a lateral drift of 2 mm in the third course above the bottom on the left end. Vertical cracks developed on the right side, Figure 14, along with the splitting of masonry on the right edge, Figure 15. Due to bed-joint sliding the wall underwent relatively higher drift before failure.

Wall WIVb was tested under a vertical pressure of 0.64 MPa. The wall underwent diagonal tensile cracking at a quite low drift ratio of 0.043 % (almost half the drift ratio at which the diagonal shear cracking occurred in all other walls). Bed joint sliding occurred after the formation of diagonal tension cracks, as shown in Figure 16. A number of inclined cracks were also developed on the right side portion of the wall, as shown in the Figure 16, causing severe damage in the wall as the test progressed. The test was stopped at a stage when it was felt that the diagonally cracked wedge as shown in Figure 17 might fall due to extensive damage.

Due to different failure modes as compared to all other walls, results of walls WIVa and WIVb were not included in the statistical analysis for determining various parameters quantifying the deformation capacity of the walls, since sliding produced higher displacements than for the other specimens.

Wall WIVc behaved differently from the rest of the tested walls. The wall was initially tested at a pre-compression level of 0.42 MPa. During the force controlled testing phase, a vertical crack appeared at the bottom during the first cycle. In the remaining two cycles, the crack propagated in the upward direction until it reached the top surface of the wall, dividing the wall in almost two parts. However, no additional crack developed till an imposed lateral displacement of 3.0 mm, Figure 18. Test was stopped at this stage and restarted at pre-compression level of 0.64 MPa. At a lateral displacement of 3.5 mm, another vertical crack, branching from the existing vertical

crack, developed and instantaneously reached the top surface of wall. The first diagonal crack developed at a displacement of 6.0 mm with a corresponding drift ratio of 0.66%. The test was stopped at a lateral displacement of 9.0 mm, cracks shown in Figure 19.

A careful study after the test revealed that the upper surface of the wall was very uneven, causing a significant gap between the top surface of the wall at the ends and the connected R.C. beam. The gap causing uneven distribution of vertical pressure at the top ends of the wall resulted in the complete vertical splitting of the masonry wall, as shown in Figure 20. Due to the uneven distribution of vertical stresses the data of the wall was not used in the study

The hysteresis loops of all the tested walls along with envelopes and bi-linear idealized curves developed by using the method proposed by Magenes and Calvi [13] discussed in sub-section 3.2.1 are shown in Figures 21 through 29. The point on envelope shown by a larger solid circle corresponds to the formation of first significant crack, defined as the crack which produced significant reduction in the lateral stiffness of the wall. A larger solid rectangular point on the envelope curve corresponded to the first diagonal tension shear crack. Envelopes with no solid circular point indicate that the first diagonal tension shear crack was also the first significant crack

Lateral forces at various distress levels in walls, namely first significant cracking (V_{fcr}), first diagonal tension cracking (V_{dcr}), maximum resistance (V_{max}), and minimum resistance along the degrading portion of lateral force-displacement curve (V_{min}), are summarized in Table 3. The lateral strengths of most of the walls were approximately same for both directions of loading.

3. Analysis of tests results

3.1 Diagonal tensile shear strength

A criterion which is often reported in the literature [14 and 15] to evaluate the shear strength (τ_d) associated to diagonal cracking for URM masonry walls is the following equation as proposed by Turnšek and Sheppard [16]:

$$\frac{V_d}{A} = \tau_d = \frac{f_{tu}}{b}\sqrt{1+\frac{\sigma_o}{f_{tu}}} \quad \text{.....} \quad (3)$$

Where b = shear correction factor which accounts for the distribution of shear stresses along the length of wall. In this work the simplified expression for coefficient b proposed by Benedetti and Tomaževic [17] is adopted: b = 1 for $h/l \leq 1.0$, b = h/l for $1.0 < h/l < 1.5$ and b = 1.5 for $h/l \geq 1.5$.

The mean tensile strength, f_{tu}, obtained from diagonal compression tests (Table 2) has been used in equation (3) and the results obtained have been compared with the experimental values of the shear strengths of the tested walls, as shown in Figure 22. Equation (3) in average estimates the shear strength of the URBM walls with reasonable accuracy for most of the tested walls.

3.2 Evaluation of displacement based properties of URBM walls from quasi-static cyclic tests

3.2.1 Displacement ductility factor

Bi-linear idealization approach of the lateral force-displacement curve proposed by Magenes and Calvi [13], as

shown in the Figure 23, was used for determining the displacement ductility factors of walls. The displacement ductility factor for an URM wall, μ_w, using the recommended criteria, can be calculated by using the relation:

$$\mu_w = \frac{d_u}{d_y} \quad \text{.....} \quad (4)$$

Where d_y = Lateral displacement at the top of a wall at the elastic limit = V_u / K_e in which V_u = 0.9 V_{max} (V_{max} = the maximum resistance of the wall in the lateral direction); K_e = elastic stiffness of the wall = $0.75V_u$/ $d_{0.75Vu}$ ($d_{0.75Vu}$ = the displacement corresponding to $0.75V_u$); and d_u = Lateral displacement at the top of the wall when the experimental lateral force V drops by 20% of V_u along the degrading curve, as shown in Figure 23. The lateral force-displacement data used for determining μ_w and other relevant properties corresponded to the first cycle of loading.

It is worth mentioning that in case of all the walls, except wall WIVa, the test was stopped due to extensive damage before the lateral force reduced to $0.8V_u$ after the post peak response. Consequently, calculation of displacement ductility factor was based on the displacement at the end of testing rather than the criteria of displacement corresponding to 0.8 V_u. This can also be seen from the results of tested walls given in Table 4. where V_{min}/ V_u > 0.8 for all the walls, except WIVa. Displacement ductility factors of the tested walls are given in Table 4. The average value of μ_w for tested walls was found to be 6.31 with a C.O.V. of 26.3%. It is important to note that for the purpose of conservativeness, the lower of the two values of μ_w for each direction of loading of a tested wall was adopted

The work carried out by Vasconcelos [18] on the influence of pre-compression level on displacement ductility factor was also re-investigated. Vasconcelos [18] reported that the displacement ductility factors for URM walls decrease with the increase in pre-compression level. In order to validate this observation, regression analysis values was carried out using the displacement ductility factors of walls belonging to WII and WIII series (having the same geometry) and corresponding pre-compression, as shown in Figure 24. However, no correlation was found between displacement ductility factor and pre-compression level as indicated by the coefficient of determination, r^2, which was as low as 0.0012. However, a better correlation was found between drift ratio at ultimate limit state and pre-compression level (r^2 = 0.497), as shown in Figure 25. Since these findings are based on limited data, no general conclusion can be drawn here, and further tests in this regard will aid to a better understanding of the phenomena.

3.2.2 Modulus of rigidity

An approach based on the results of quasi-static cyclic tests of walls was followed to determine the modulus of rigidity G_m of masonry. Using this approach, G_m is calculated by considering the elastic stiffness of the idealized bi-linear lateral force-displacement curve of the wall, as shown in Figure 23, with the classical structural analysis approach using following relation**:**

$$d_y = \frac{V_u.h^3}{12E_mI} + \frac{1.2V_u.h}{G_mA} \quad \text{.....} \quad (5)$$

Values of G_m for tested walls, solving Equation 5 for G_m, were determined using the average value of E_m = 1300 MPa obtained from prism tests (Table 1). The average values of G_m and G_m/E_m were found to be 679 MPa and 0.47, respectively, with a C.O.V. of 19.8 %.

3.2.3 Energy dissipation

Unreinforced masonry when loaded in inelastic range undergoes macro cracking. The energy is dissipated due to the release of fracture energy. The subsequent friction of cracked surfaces over each other further increases energy dissipation. The dissipation of energy in a normalized quantified way is determined by calculating the "coefficient of equivalent viscous damping" (ξ_{eq}) using the following equation.

$$\xi_{eq} = \frac{E_d}{2\pi E_i} \quad \text{.....} \quad (6)$$

where E_i = energy required in one cycle to impose a target lateral force/displacement in the wall and is determined by computing the area of force-displacement diagram, both in positive and negative loading directions, as shown in Figure 26a; and E_d = Energy dissipated in one cycle of imposed lateral force/displacement and is determined by computing the areas under the positive and negative branches of force displacement hysteresis loops, as shown in fig 26b [18].

Variation in the coefficient of equivalent viscous damping with the increase in the drift ratios for the tested walls is shown in Figures 27. The general trend, as observed from Figure 27, was that the coefficient of equivalent viscous damping of the walls increases at a higher rate after the flexural-tensile cracking in the bed joint (corresponding drift ratio, δ= 0.05%) till the initiation of diagonal tensile shear cracking (δ=0.1%). ξ_{eq} increased at a comparatively lower rate after the initiation of diagonal tensile cracking till the peak resistance of walls (δ=0.2%). Only a slight increase of the coefficient of equivalent viscous damping is visible after the walls attained their peak resistance.

The coefficient of equivalent viscous damping, ξ_{eq}, of slender walls (WIc) before diagonal tensile shear cracking was found to be relatively lower as compared to other walls, as shown in Figure 27. One of the possible reasons for this behaviour may be higher flexural deformation in slender walls which tends to give a less dissipative behaviour.

Similarly, coefficient of equivalent viscous damping for squat walls (WIV series) was relatively higher as compared to other walls. This may be attributed to high dissipation of energy due to friction caused by bed joint sliding.

The effect of pre-compression on ξ_{eq} was also investigated and graphically shown in Figure 28. As shown in Figure 28, an increase in the pre-compression results in a decrease in the coefficient of equivalent viscous damping in the post peak response (δ = 0.2%).

4. Performance based limit states

Performance of structural elements / structures based on inter-story drifts is the backbone of performance-based concepts, as for instance proposed, for the case of URM buildings, in FEMA 356 [3].A criterion for performance based evaluation of URM walls failing in shear was sought as a part of this study. Table 5 summarizes the mean values of E_d/E_i and ξ_{eq} for various limit states which were used as basis for various proposed performance levels. Mean value of E_d/E_i (or ξ_{eq}) corresponding to a particular limit sates was calculated as follows:

$$\left(\frac{E_d}{E_i}\right)_{mean} = \frac{\sum_n \left(\frac{E_d}{E_i}\right)}{n} \quad \text{.....} \quad (7)$$

Where n is the total number of cycles imposed in the particular limit state.

Normally three performance levels are defined for performance based evaluation, namely, Immediate occupancy (IO), life safety (LS) and collapse prevention (CP). Based on their definitions they can be related to various levels of limit sates. As a first consideration, IO performance level can be related to a drift ratio corresponding to the formation of first diagonal tension shear crack. During the experiments the diagonal tension shear cracks in a wall just after their formations were too narrow to be seen and the wall still maintained most of its integrity. Average value of drift ratio just at the formation of diagonal tensile cracking was found to be 0.087% with a C.O.V of 8.2 %. Similarly, LS performance level can be related to a drift ratio when the wall just attains its maximum resistance. The diagonal cracks were widened and easily seen at this stage. In some cases, additional minor cracks were also observed. However, the wall was still considered as economically repairable. Average value of drift ratio at maximum resistance was found to be 0.22% with a C.O.V of 32.8%. Finally, it was observed during the test that, in spite of extensive damage in post peak response corresponding to the final stages of testing, the walls were still able to withstand vertical load and did not collapse. However, the distributed and widened cracks in the walls were not feasible for repair. Drift ratio at a stage when shear resistance drops to 80% of V_u can be established as a basis for CP performance level. Mean value of drift ratio at this level was found to be 0.52% with a C.O.V of 39.4%.

Given the scatter in the drift ratios corresponding to the different performance levels, a safe rounding off to 0.08%, 0.2% and 0.4% respectively for the IO, LS and CP performance levels could be accepted. Such drift limits are slightly lower than the drift limits proposed in FEMA 356 for URM masonry failing in shear. Nevertheless, they seem to lie within the ranges that have been reported from experimental researches on solid brick masonry. It must be recalled that specific masonry typologies can have widely different deformation capacity depending on the type of units and mortars that are used, and the drift values presented in this work can be considered appropriate for the typology being considered (solid brick with stone dust mortar).

5. Conclusions and recommendations

Based on the experimental seismic performance investigation carried out on URBM walls built with stone dust (*Khaka)* mortar, the following conclusions can be made:

1. Shear failure was the mechanism of interest and the specimens were designed to display such failure type; diagonal tension shear cracking was the dominant failure mode for the walls having aspect ratios of 0.94 and 1.22. Walls with aspect ratio of 0.66 underwent diagonal tension shear cracking followed by bed-joint sliding
2. The pre-compression level has an influence on the cracking pattern of the walls having same aspect ratio but different pre-compression levels. Higher the pre-compression level, greater were the number of cracks with relatively narrow width
3. The tests were stopped in almost all walls due to severe damage in the final stages of testing without significant degradation of lateral force after the walls gained their maximum resistance.

4. The strength criterion by Turnšek and Sheppard seems to provide acceptable conservative estimates of the shear strength for most of the tested URBM walls, provided the principal tensile strength of masonry from diagonal compression tests is determined by using RILEM Equation. In the absence of diagonal compression tests the principal tensile strength of masonry may be calculated from Turnšek and Sheppard equation due to its accuracy.
5. Values of G_m/E_m from quasi-static cyclic tests on masonry walls were found to be satisfactory. Average value of G_m and G_m/E_m determined from these tests were 690 MPa and 0.47, respectively with C.O.V of 19.8%. Modulus of rigidity of brick masonry in the field practice may be calculated by using the relation: $G_m = 0.4E_m$.
6. No correlation was found between displacement ductility factors and pre-compression levels from statistical regression analysis. Relatively better correlation was found between drift ratio at ultimate limit state and pre-compression level. However, these statistical findings correspond to limited data. Additional experimental work may be conducted to investigate the influence of pre-compression levels on ductility factors and ultimate drift ratio.
7. By comparing the results of walls with same aspect ratio but different pre-compression levels, it is concluded that an increase in the pre-compression caused reduction in coefficient of equivalent viscous damping in post peak response of the walls.
8. Mean value of drift ratios corresponding to IO, LS and CP performance levels (for walls failing in shear) is found to be 0.087% ,0.22% and 0.52%, respectively with C.O.V of 8.2%, 39.4%. and 39.4%. For use in field practice the drift ratios corresponding to IO, LS and CP performance levels, for walls failing in shear, may be taken as 0.08% ,0.2% and 0.4%, respectively.

Acknowledgments

The first author is grateful to the University of Engineering and Technology, for granting him study leave during his PhD studies to carry out the experimental work and the Higher Education Commission (HEC) for providing funds for his research project. The first author is also grateful to Prof. Dr. Junwu Dai at I.E.M., Harbin, China who managed to arrange this experimental work at I.E.M. Thanks are also due to Mr. Feng, graduate student at I.E.M., who facilitated him during the experimental work.

References

[1] Javed, M., Naeem, A., Penna, A. and Magenes, G. [2006] Behaviour of masonry structures during the Kashmir 2005 earthquake. Paper no.1077, Proceedings of the First European Conference on Earthquake Engineering and Seismology, Geneva, Switzerland.

[2] Javed, M. [2009] Seismic risk assessment of unreinforced brick masonry building systems of Northern Pakistan, Ph.D. thesis, Civil Engineering Dept., NWFP University of Engineering and Technology, Peshawar, Pakistan

[3] FEMA 356 [2000] Prestandard and Commentary for the Seismic Rehabilitation of Buildings, ASCE-FEMA, Washington

[4] ASCE-SEI 41-06, [2007] Seismic Rehabilitation of Existing Buildings. ASCE – SEI, Reston Virginia

[5] CEN [2005] Eurocode 8: Design of structures for earthquake resistance - Part 3: Assessment and retrofitting of buildings,", EN 1998-3, Brussels, Belgium.

[6] Bosiljkov, V., Page, A., Bokan-Bosiljkove, V. and Zarnic, R. [2003] Performance based studies of in-plane loaded unreinforced masonry walls. Masonry International;16:39-50.

[7] Ali, Q. [2004] Seismic performance study of brick masonry building systems in Peshawar region, Ph.D. thesis, Civil Engineering Dept., NWFP University of Engineering and Technology, Peshawar, Pakistan, 2004

[8] ASTM C1314 - 11 [2002] Standard Test Method for Compressive Strength of Masonry Prisms, American Society for Testing and Materials, Philadelphia, USA.

[9] ASTM, E 519-02 [2002] Standard Test Method for Diagonal Tension (Shear) in Masonry Assemblages, American Society for Testing and Materials, Philadelphia, USA.

[10] RILEM. LUM B6 [1994] Diagonal tensile strength tests of small wall specimens. Tech Rep, RILEM.

[11] EN-1052-3 [2002] Methods of test for masonry – Part 3: Determination of initial shear strength, Brussels, Belgium.

[12] Popov.E.P., and Balan T.A. [1998] Engineering mechanics of solids. Second edition, (Prentice Hall publishers, New Jersey).

[13] Magenes, G. and Calvi, G.M. [1997] In-plane seismic response of brick masonry walls, Earthquake Engineering and Structural Dynamics, 26, pp. 1091-112.

[14] Tomaževic,M. [1999] Earthquake-resistant design of masonry buildings, (Imperial College Press, London).

[15] Tomaževic,M. [2009] Shear resistance of masonry walls and Eurocode 6: shear versus tensile strength of masonry Materials and Structures, vol. 42:889–907 (DOI 10.1617/s11527-008-9430-6).

[16] Turnšek V. and Sheppard P.[1980] The shear and flexural resistance of masonry walls. Proceedings of International Research Conference on Earthquake Engineering, Skopje.

[17] Benedetti D. and Tomaževic M. [1984] Sulla verifica sismica di costruzioni in muratura (on the seismic assessment of masonry structures),Ingegneria Sismica, **I**(0), pp. 9–16 (in Italian).

[18] Vasconcelos G. [2004] Experimental investigations on the mechanics of stone masonry: Characterization of granites and behaviour of ancient masonry shear walls, PhD. thesis, University of Minho, Portugal.

Figure 1 Typical arrangement of displacement dials gages for determining vertical deformations in a masonry prism.

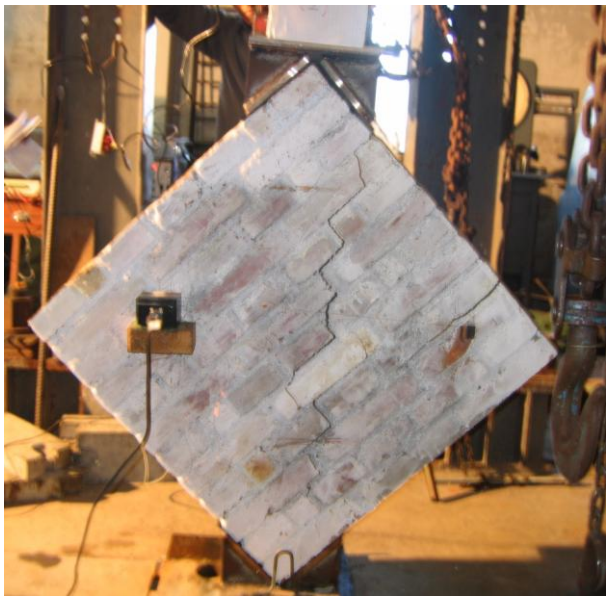

Figure 2 Testing setup used for conducting diagonal compression tests

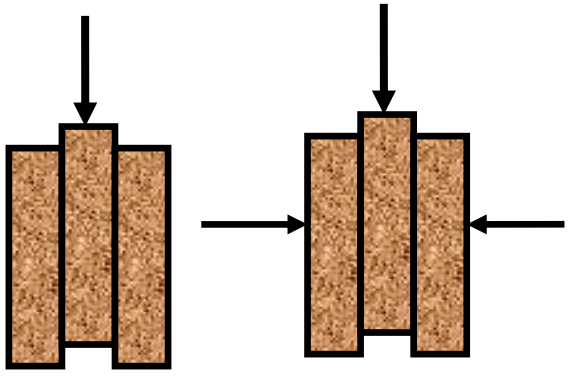

(a) (b

Figure 3 Testing arrangement for carrying out triplet tests

(a) Specimen without pre-compression
(b) Specimen with pre-compression applied horizontally

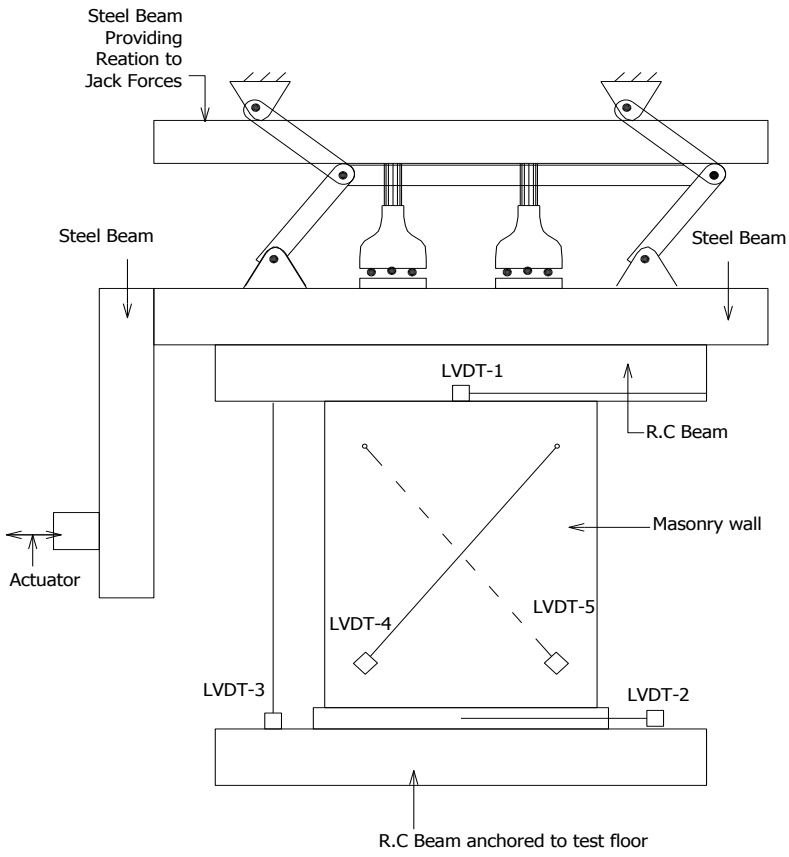

Figure 4 Testing setup used for conducting in-plane quasi-static cyclic tests on URBM walls

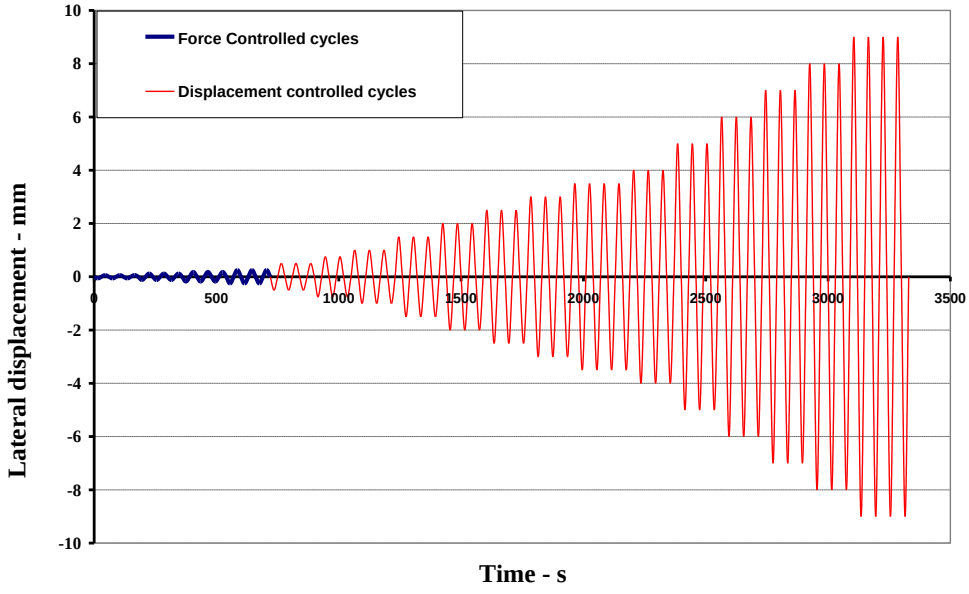

Figure 5 displacement history imposed on the walls top during quasi-static cyclic tests

Figure 6 Wall WIc at end of testing showing diagonal and vertical cracks.

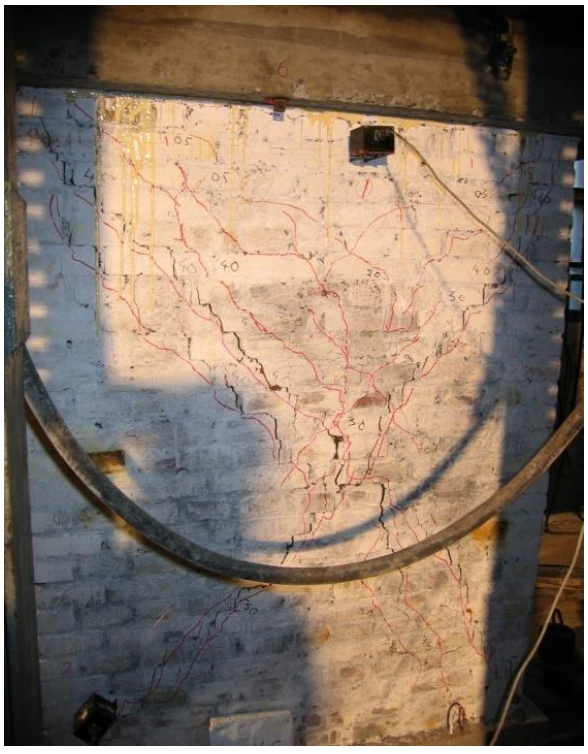

Figure 7 Multiple inclined cracks along each diagonal of wall WIb

Figure 8 Separation of diagonally cracked 'wedge' on the left end of wall WIIb at the end of testing

Figure 9 Extensive sliding of damaged 'wedge' on the right end of wall WIIa

Figure 10 Multiple inclined cracks along each loading direction in wall WIIIa.

Figure 11 Vertical cracks along both the ends of wall WIIIb

Figure 12 Vertical splitting of masonry and crushing of bricks in wall WIIIa.

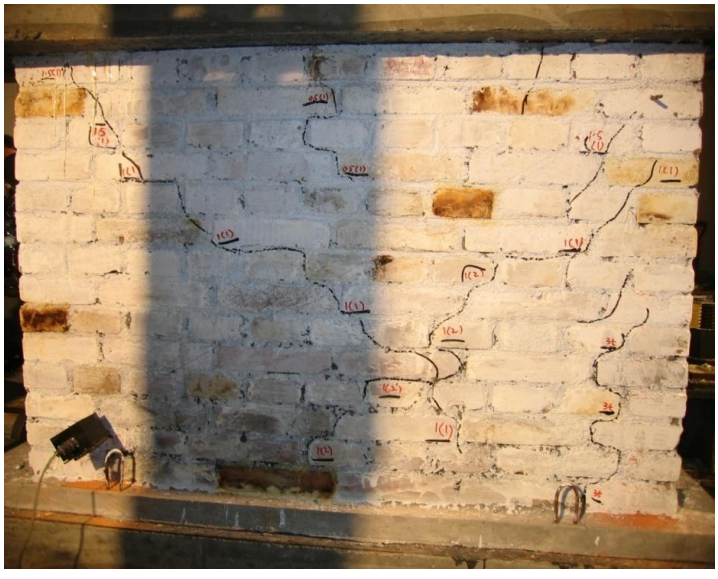

Figure 13 Wall WIVa just before failure of epoxy bond between foundation beam of wall and R.C. beam anchored to the testing floor

Figure 14 Wall WIVa at test completion showing extensive damage to brick units and vertical cracks at the right side

Figure 15 Vertical splitting of masonry across all the head joints of wall WIVa

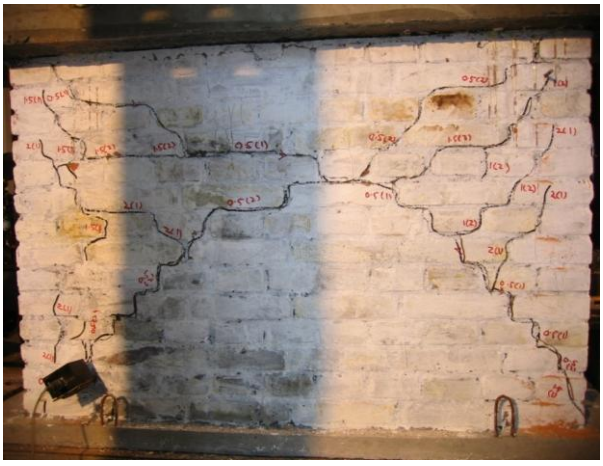

Figure 16 Bed joint sliding in wall WIVb at fourth layer from top end of wall. Note the formation of multiple inclined cracks.

Figure 17 Separation of diagonally cracked 'wedge' due to the formation of multiple inclined cracks on the right end of wall WIVb.

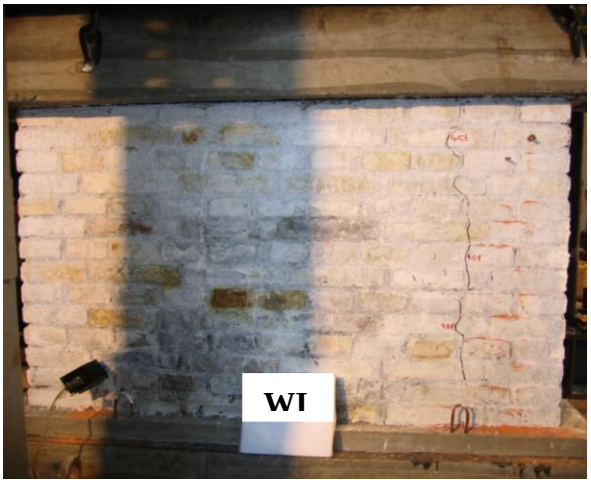

Figure 18 Wall WIVc at the end of test under a pre-compression of 0.42 MPa

Figure 19 Wall WIVc after testing under a pre-compression of 0.64 MPa

Figure 20 Splitting of masonry in wall WIVc due to the concentration of vertical stresses at the right end

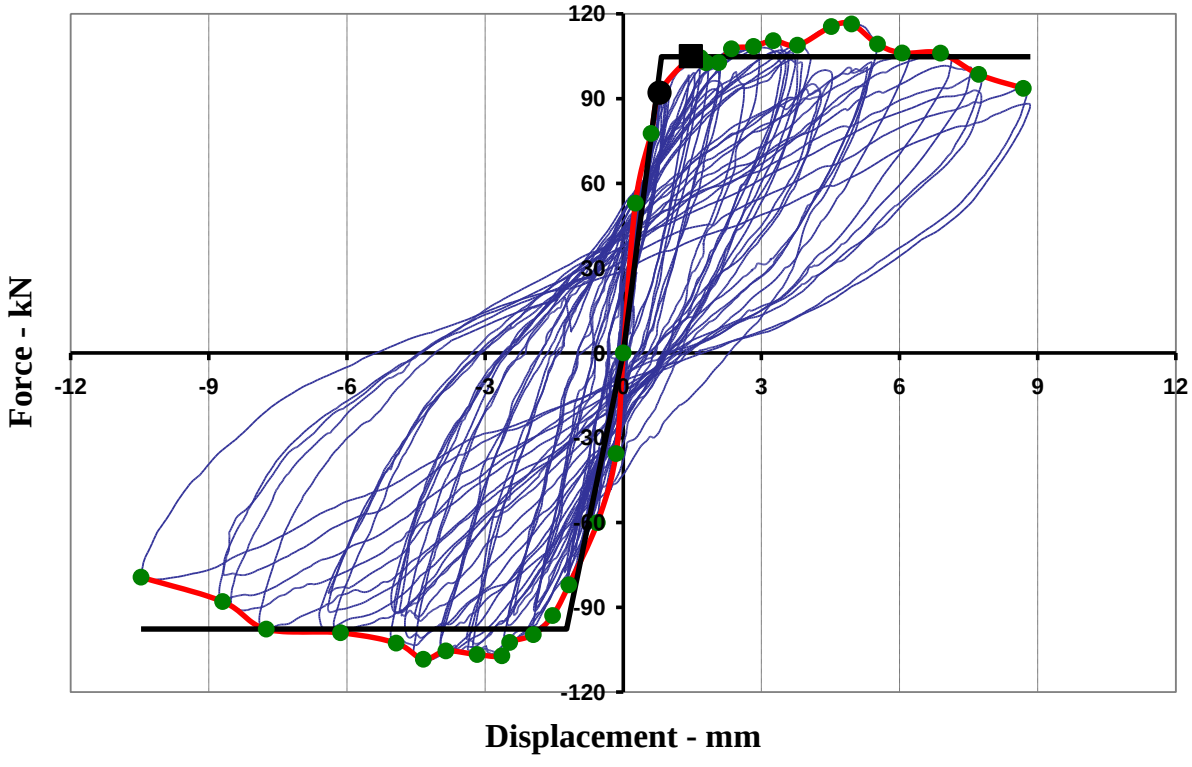

(a) Wall WIc

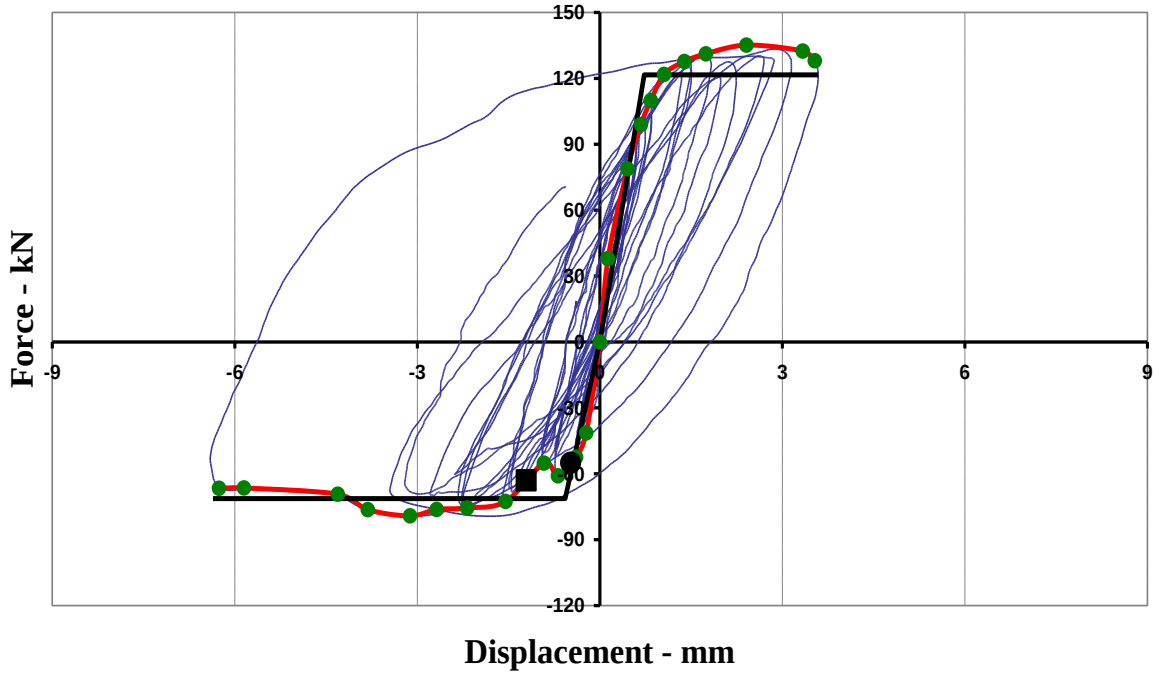

(b) Wall WIIa

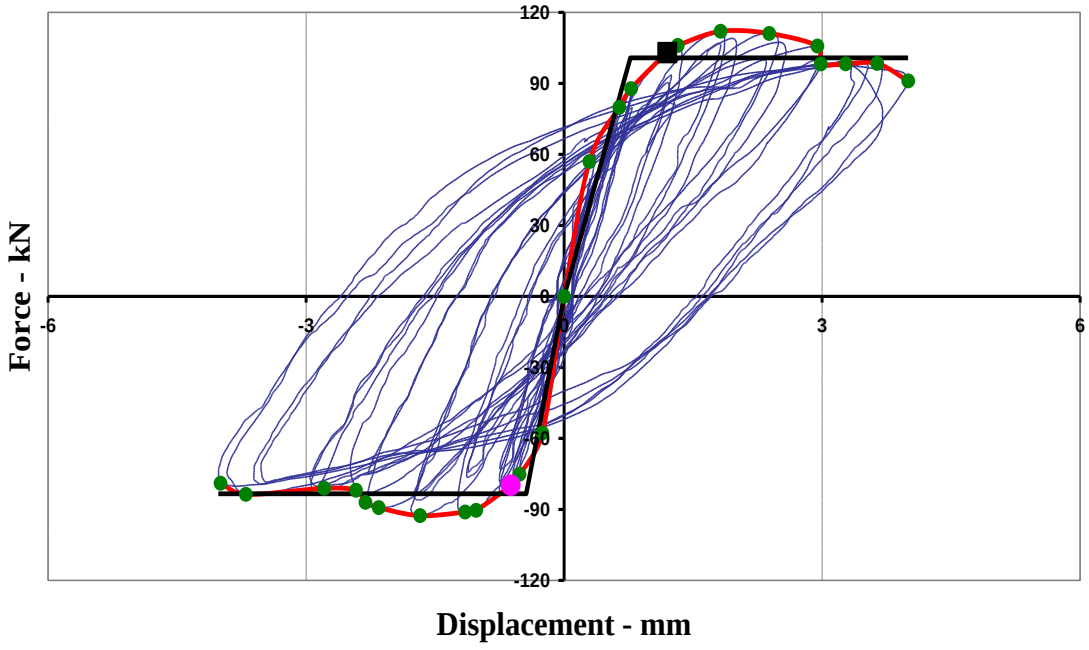

(c) Wall WIIb

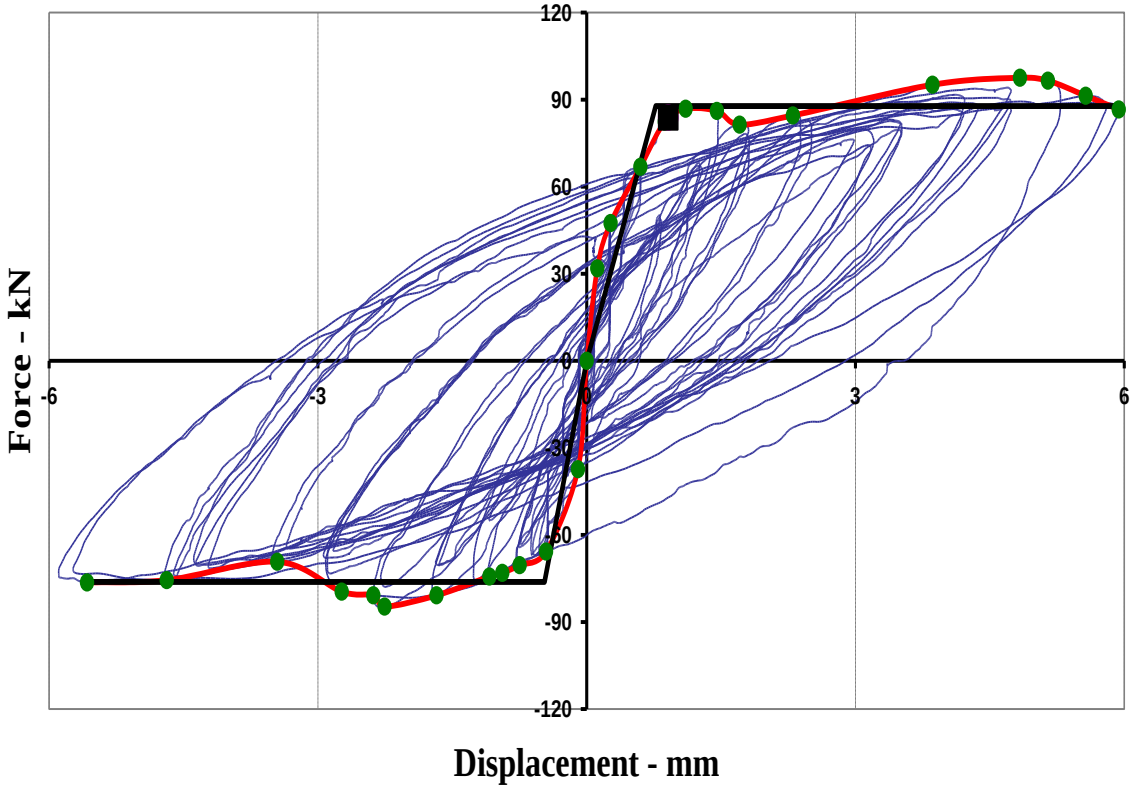

(d) Wall WIIc

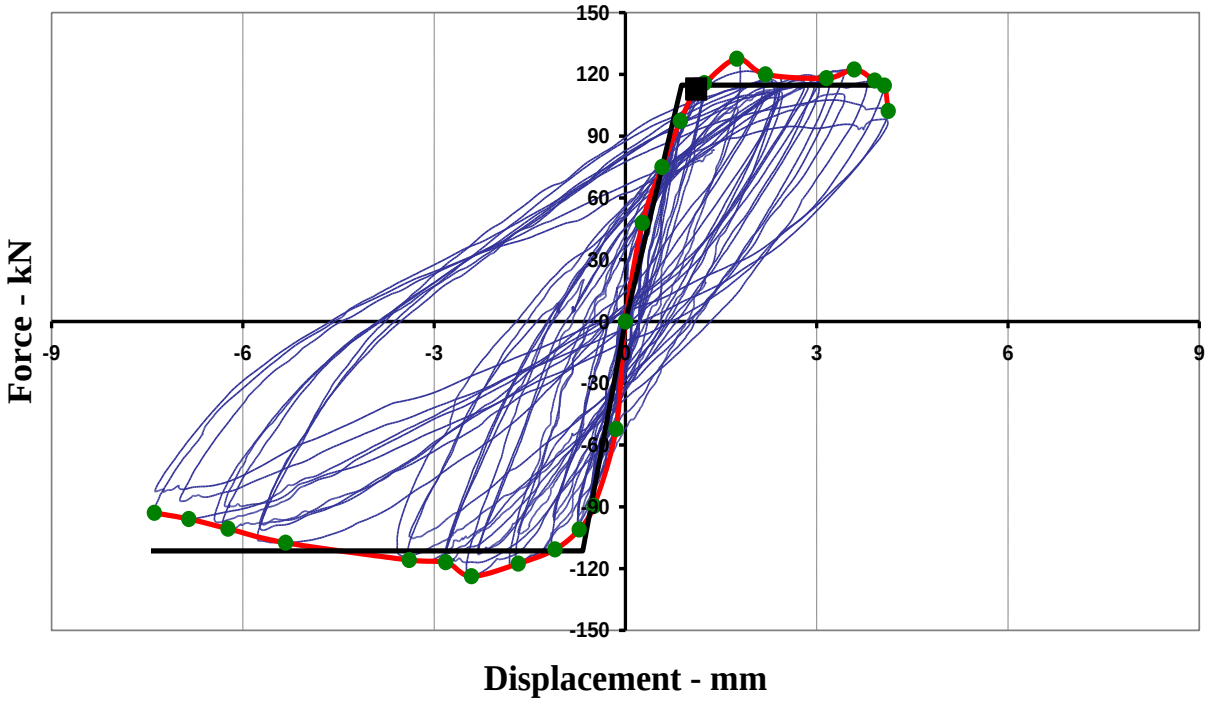

(e) Wall WIIIa

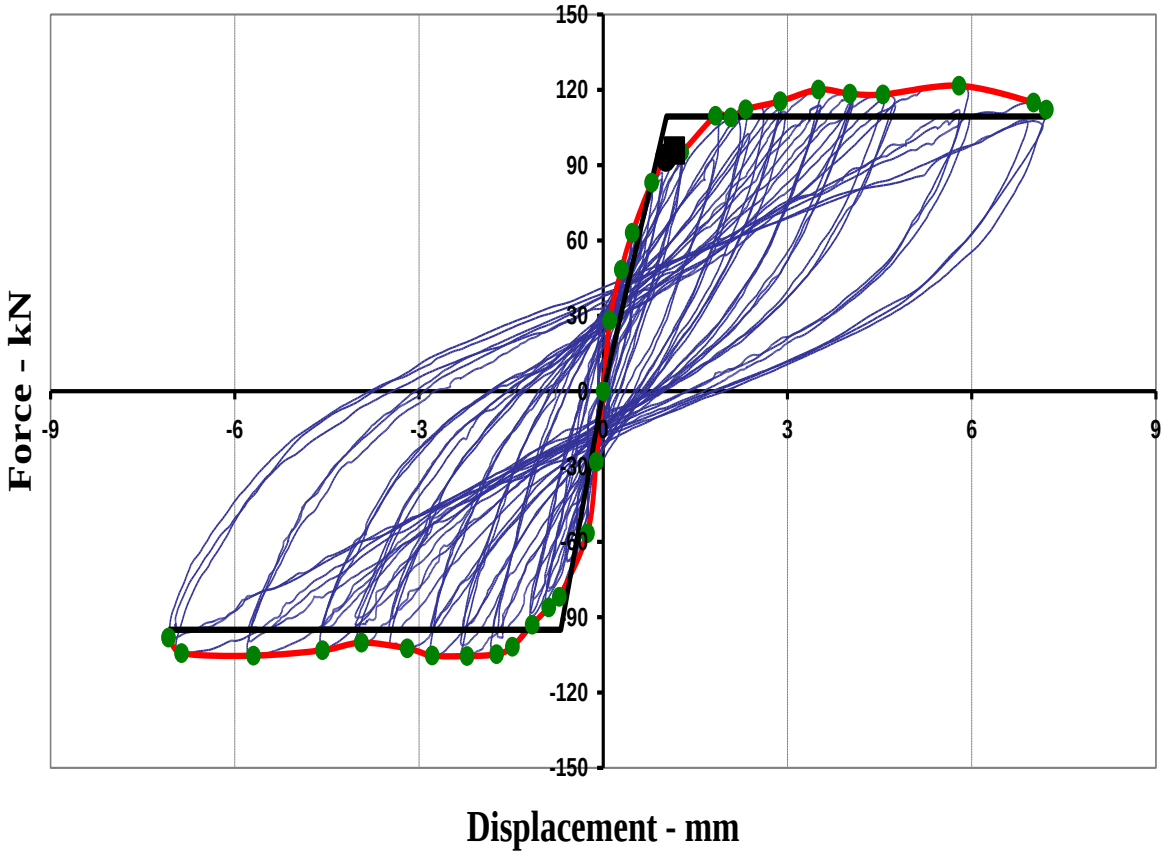

(f) Wall WIIIb

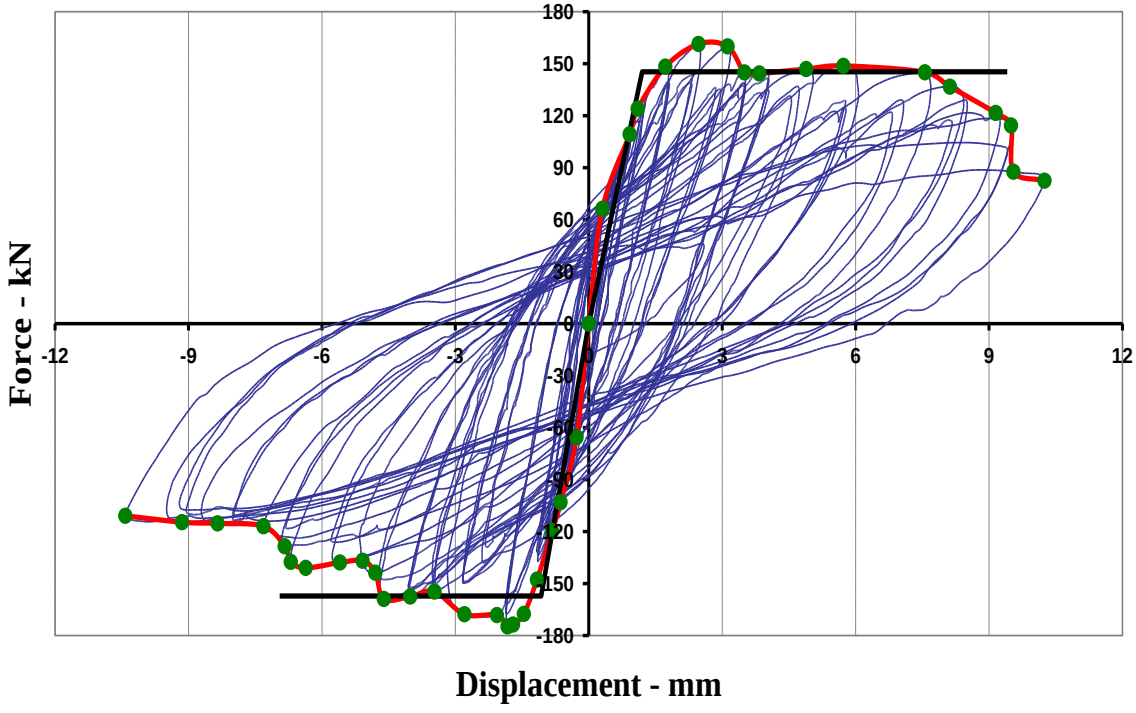

(g) Wall WIVa

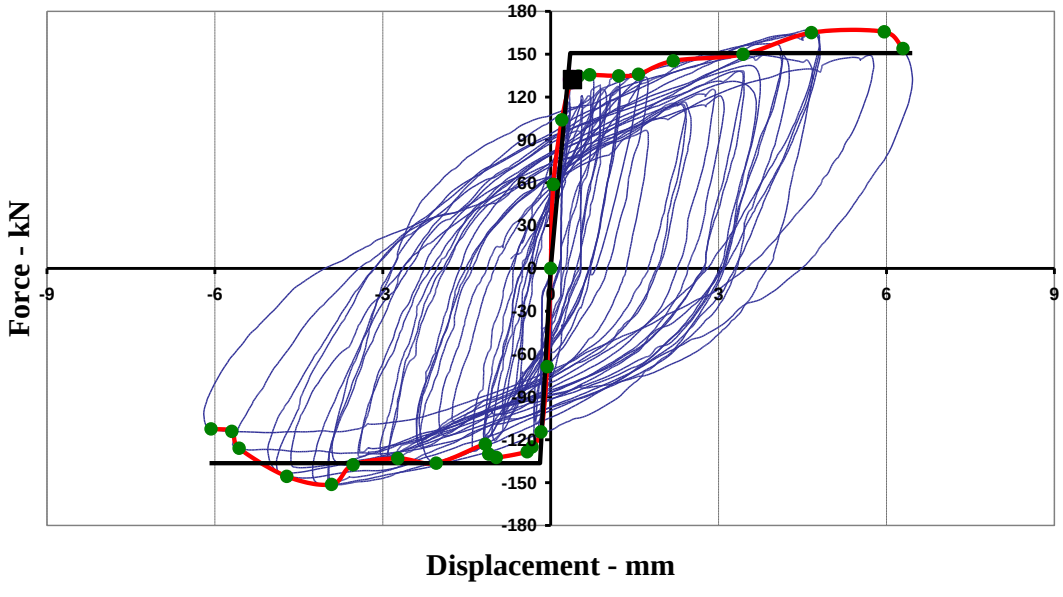

(h) Wall WIVb

Figure 21 a through h: Hysteresis loops, envelopes and bi-linear idealized curves of the walls

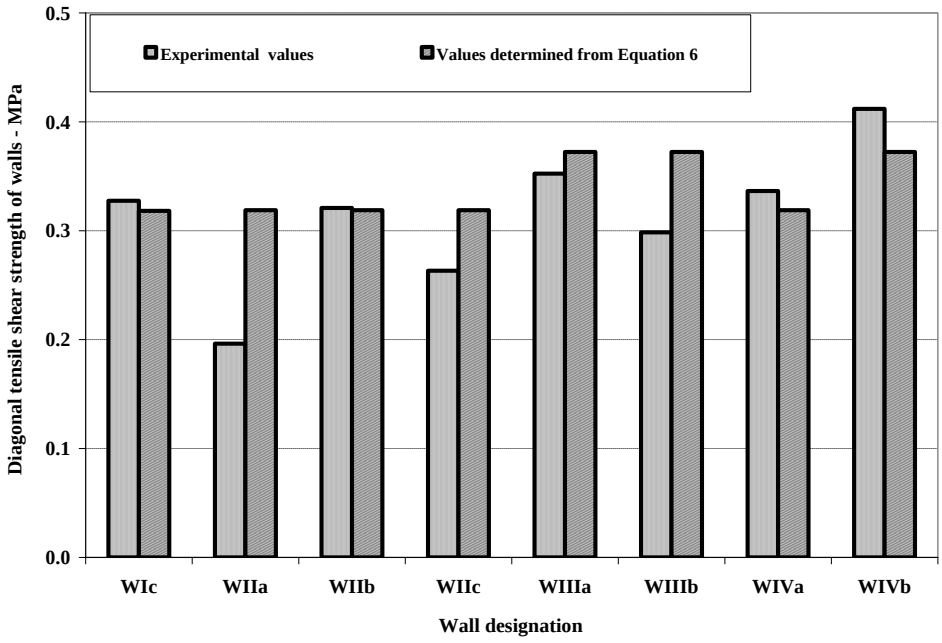

Figure 22 Comparison of diagonal tensile shear strength of walls from experimental work with Equation 6.

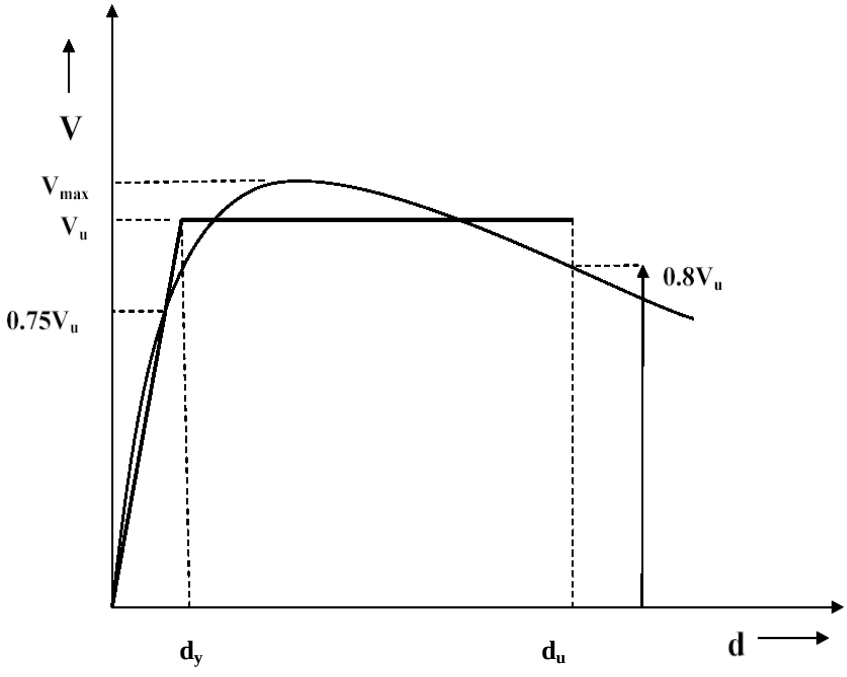

Figure 23. Bi-linear idealization of URM walls

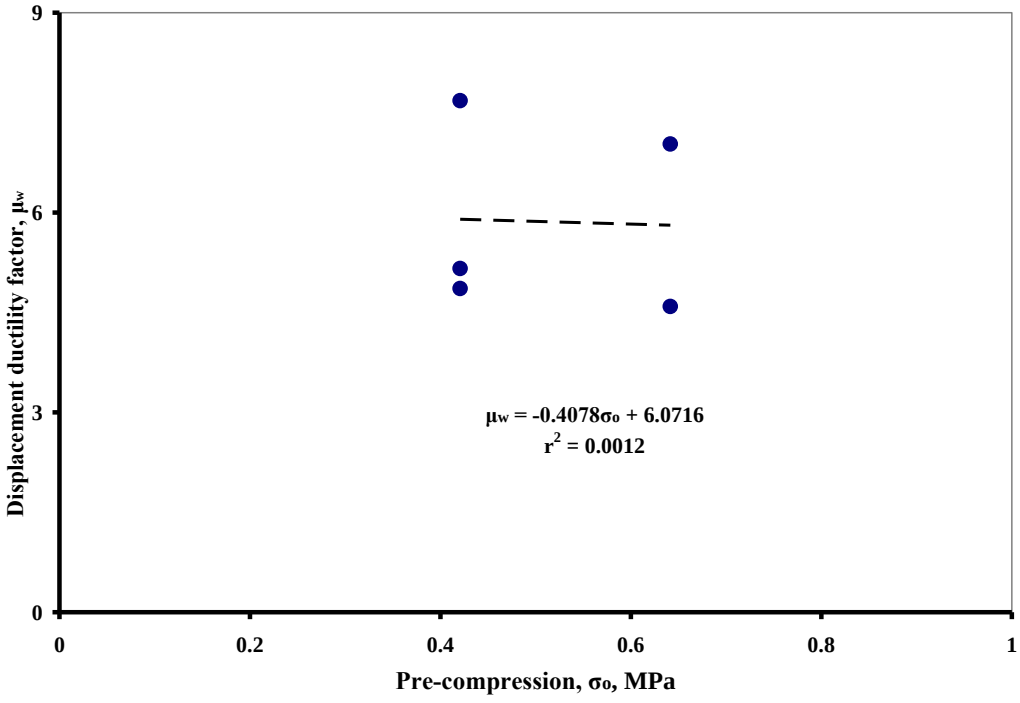

Figure 24 Effect of Pre-compression on displacement ductility factors.

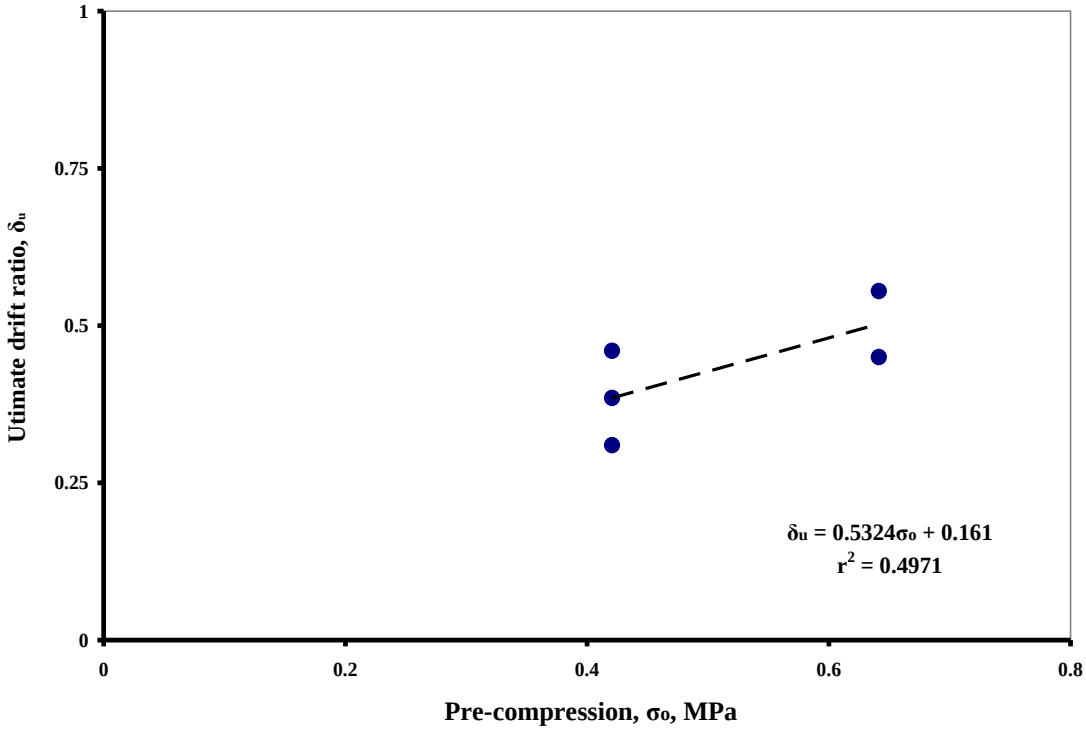

Figure 25 Effect of Pre-compression on ultimate drift ratio.

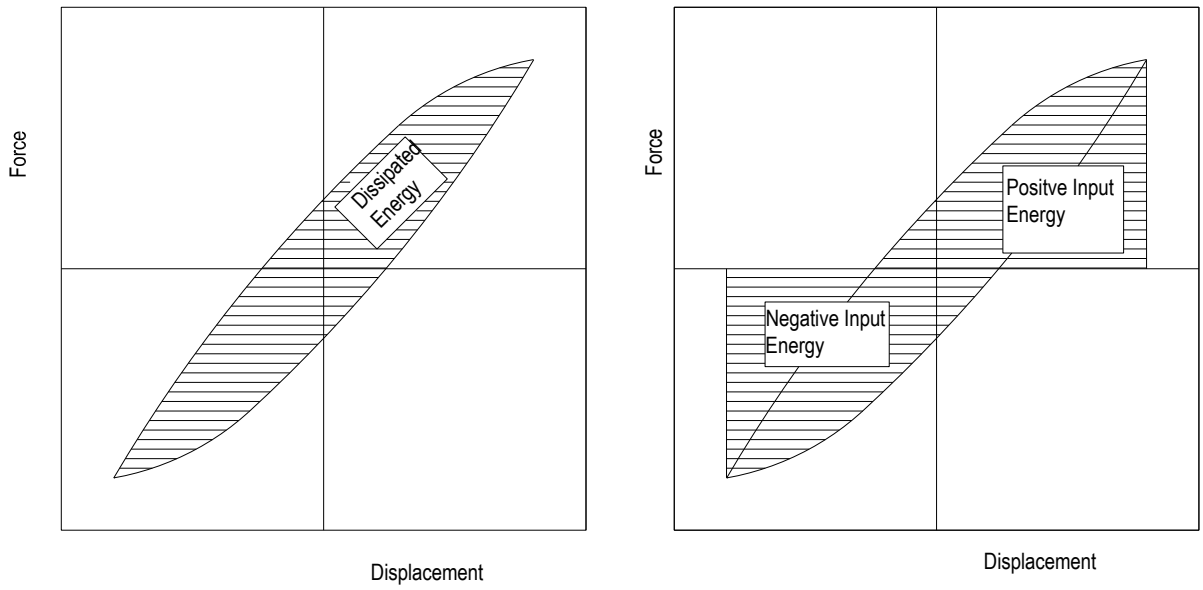

Figure 26 Energy determination in one cycle of loading [Va 04] a. Dissipated energy b. Input energy

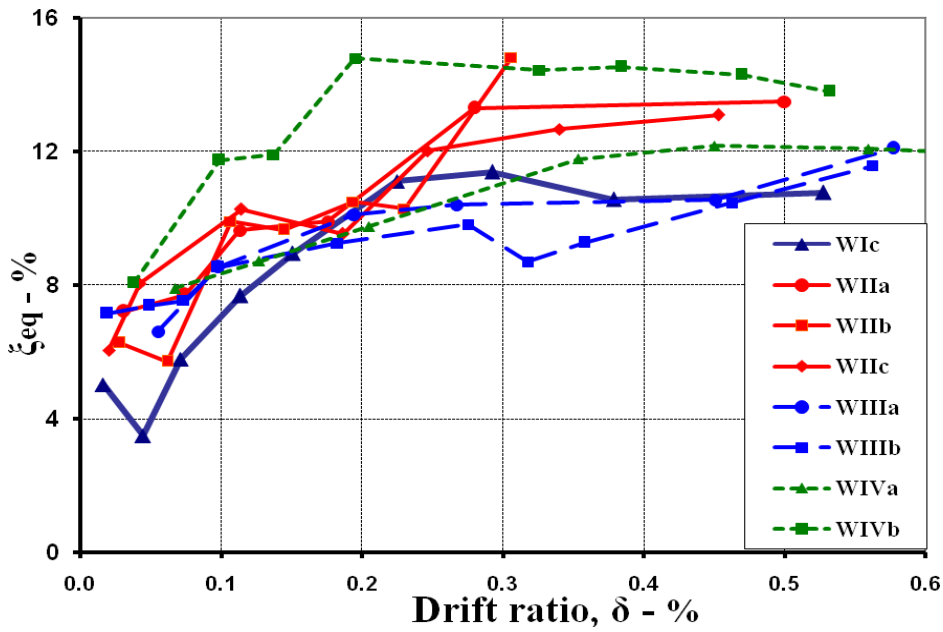

Figure 27 Variation in coefficient of equivalent viscous damping with the increase in drift ratio.

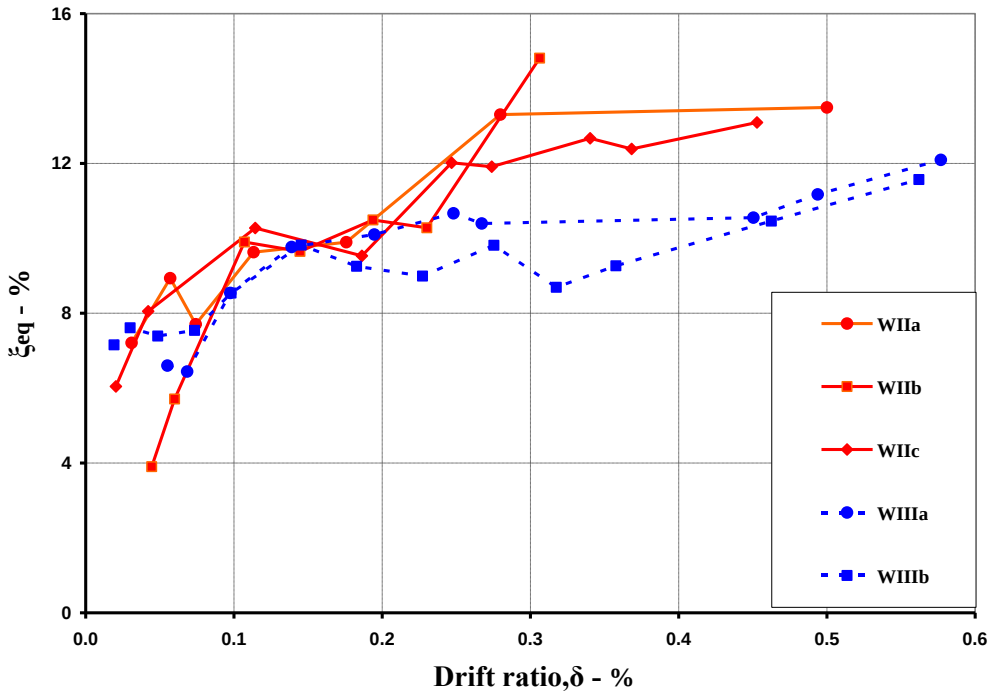

Figure 28 Influence of the pre-compression levels on the coefficient of equivalent viscous damping(All the walls have same aspect ratios).

Table 1. Mechanical Property of masonry and its constituents used in the experimental work

	Mean value	No of tested specimens	C.O.V (%)
Compressive strength of brick units perpendicular to the bed joint (MPa), f_b	22.5	12	23.4
Tensile strength of the brick units (MPa), f_{bt}	2.67	8	22.2
28 days Compressive strength of the mortar cubes (MPa), f_{mo}	5.05	24	10.3
Compressive strength of the masonry (MPa), f_m	4.53	9	14.2
Principal Tensile strength of the masonry (MPa), f_{tu}	0.24	4	16.7
Coefficient of friction of masonry, μ	0.59	11	-
Cohesion of masonry (MPa), c	0.39	11	-
Modulus of elasticity of the masonry (MPa) , E_m	1300	9	17

Table 2: Characteristics of tested walls

Wall Series	h (mm)	l (mm)	t (mm)	A.R= h/l	σ_o (MPa)	σ_o/ f_m
WI	1660	1360	236	1.22	0.71	0.153
WII	1280	1360	236	0.94	0.42	0.091
WIII	1280	1360	236	0.94	0.64	0.138
WIV	900	1360	236	0.66	0.64	0.138

Table 3. Lateral forces in walls corresponding to various stages of testing and moduli of rigidities

Wall	Loading Direction	V_{fcr} (kN)	V_{dcr} (kN)	V_{max} (kN)	V_{min} (kN)	G_m (Mpa)	G_m/E_m	Failure Mode
WIc	+	92.1	105.0	116.4	83.8	783	0.55	Diagonal Tension
	-	-	-	108.4	78.2	492	0.34	
WIIa	+	-	63.0	135.1	97.3	796	0.56	Diagonal Tension
	-	55.0	-	79.2	57.0	599	0.42	
WIIb	+	-	103.0	112.0	80.6	620	0.43	Diagonal Tension
	-	79.8	-	92.6	66.7	903	0.63	
WIIc	+	83.8	83.8	97.6	70.3	540	0.38	Diagonal Tension
	-	-	-	84.7	61.0	778	0.54	
WIIIa	+	112.9	112.9	127.6	91.9	621	0.43	Diagonal Tension
	-			123.7	89.1	796	0.56	
WIIIb	+	93.0	95.8	120.1	87.6	507	0.36	Diagonal Tension
	-	-	-	105.5	76.0	652	0.46	
WIVa at 0.42 Mpa	+	113.2	113.2	-	-	-	-	-------
	-	-	-	-	-	-	-	
WIVa at 0.64 Mpa	+	-	-	161.4	116.2	405	0.28	Diagonal Tension followed by Bed joint sliding
	-	-	-	173.6	125.8	493	0.34	
WIVb	+	132.2	132.2	165.1	120.6	1455	1.02	Diagonal Tension followed by Bed joint sliding
	-	-	-	151.3	109.1	2445	1.71	

Table 4. Displacement ductility factors for tested wall specimens

Wall designation	Loading direction	V_u (kN)	V_{min}/V_u	K_e (kN/mm)	d_y (mm)	d_u (mm)	δ_u (%)	μ_w
WIc	+	104.8	0.89*	125	0.83	8.84	0.53	10.69
	-	97.7	0.81*	80	1.23	10.47	0.63	8.54
WIIa	+	121.6	1.05*	165	0.73	3.59	0.28	4.86
	-	71.3	0.93*	128	0.57	6.36	0.49	11.03
WIIb	+	100.8	0.90*	132	0.77	4.00	0.31	5.16
	-	83.4	0.95*	193	0.44	4.02	0.31	9.09
WIIc	+	87.8	0.99*	115	0.77	5.94	0.46	7.68
	-	76.2	1.00*	158	0.47	5.89	0.46	12.62
WIIIa	+	114.8	0.89*	129	0.88	4.04	0.32	4.59
	-	111.4	0.83*	169	0.67	7.44	0.58	11.16
WIIIb	+	109.4	1.02*	105	1.03	7.22	0.56	7.03
	-	95.0	1.03*	139	0.69	7.08	0.55	10.21
WIVa	+	145.3	0.60**	122	1.20	9.41	1.05	8.71
	-	157.2	0.71**	147	1.07	6.95	0.77	7.24
WIVb	+	150.8	0.88*	424	0.35	6.47	0.72	18.66
	-	136.4	0.82*	767	0.19	6.11	0.68	32.46

* Test was stopped before lateral force reduced to 0.8 V_u
** Results of wall re-tested at a pre-compression level of 0.64 MPa

Table 5: Energy dissipation properties and coefficient of viscous damping for different limit states of tested walls

Wall No.	Diagonal tension shear cracking limit state		Max resistance limit state		Ultimate Limit state	
	Mean E_d/E_i- %	Mean ξ_{eq} - %	Mean E_d/E_i- %	Mean ξ_{eq}- %	Mean E_d/E_i- %	Mean ξ_{eq}- %
WIc	28	2.9	62	7.5	69	8.7
WIIa	45	9.4	61	16.4	76	21.9
WIIb	30	5.7	60	12.8	77	26.1
WIIc	47	10.1	53	11.7	77	23.3
WIIIa	42	9.4	48	11.0	67	17.2
WIIIb	46	11.3	57	12.5	64	13.0
WIVa	--	--	55	12.4	77	22.0
WIVb	50	13.5	88	31.3	87	33.8